

# The association between spatiotemporal coupling of default mode network and behaviors is specifically modulated by peripheral inflammation in major depressive disorder

Received: 18 December 2025

Accepted: 30 March 2026

Published online: 11 April 2026

Cite this article as: Chen J., Sun X., Yue S. *et al.* The association between spatiotemporal coupling of default mode network and behaviors is specifically modulated by peripheral inflammation in major depressive disorder. *BMC Psychiatry* (2026). <https://doi.org/10.1186/s12888-026-08045-6>

Junxia Chen, Xiaoying Sun, Suping Yue, Zibin Feng, Ruikun Yang, Yue Yu, Hui He, Suli Zhao, Yifan Li, Shuxiao Chen, Roberto Rodriguez-Labrada, Mingjun Duan, Dezhong Yao, Sisi Jiang & Cheng Luo

We are providing an unedited version of this manuscript to give early access to its findings. Before final publication, the manuscript will undergo further editing. Please note there may be errors present which affect the content, and all legal disclaimers apply.

If this paper is publishing under a Transparent Peer Review model then Peer Review reports will publish with the final article.

# **The association between spatiotemporal coupling of default mode network and behaviors is specifically modulated by peripheral inflammation in major depressive disorder**

Junxia Chen<sup>1,2</sup>, Xiaoying Sun<sup>1,2</sup>, Suping Yue<sup>1,3</sup>, Zibin Feng<sup>1,2</sup>,  
Ruikun Yang<sup>1,2</sup>, Yue Yu<sup>1,3</sup>, Hui He<sup>1,3</sup>, Suli Zhao<sup>1,2</sup>, Yifan Li<sup>1,2</sup>,  
Shuxiao Chen<sup>1,2</sup>, Roberto Rodriguez-Labrada<sup>4</sup>, Mingjun Duan<sup>1,3</sup>,  
Dezhong Yao<sup>1,2,5</sup>, Sisi Jiang<sup>1,2,5</sup>, Cheng Luo<sup>1,2,5,6\*</sup>

1. The Clinical Hospital of Chengdu Brain Science Institute, MOE Key Lab for Neuroinformation, School of Life Science and Technology, University of Electronic Science and Technology of China, Chengdu 611731, P. R. China.

2. China-Cuba Belt and Road Joint Laboratory on Neurotechnology and Brain-Apparatus Communication, University of Electronic Science and Technology of China, Chengdu, 610054, P. R. China.

3. Department of Psychiatry, The Clinical Hospital of Chengdu Brain Science Institute, University of Electronic Science and Technology of China, Chengdu 610056, P.R. China

4. Cuban Neuroscience Center, La Habana, Cuba.

5. Research Unit of NeuroInformation, Chinese Academy of Medical Sciences, 2019RU035, Chengdu, P. R. China.

6. Department of Radiology, The Fourth People's Hospital of Chengdu, Chengdu 610056, PR China.

\*E-mail address of corresponding author: chengluo@uestc.edu.cn.

## **Abstract**

**Background:** Default mode network (DMN) disruption and systemic inflammation are hallmarks of major depressive disorder (MDD), but their relationship with behavioral impairments is unclear. This study aimed to characterize DMN spatiotemporal dynamics in MDD and link them to inflammation and behavioral deficits.

**Method:** Resting-state functional magnetic resonance imaging data were obtained from 87 MDD and 104 healthy controls (HC). Periodic spatiotemporal patterns (PSTPs) were defined by the switching of anti-correlation between the DMN and task-positive network. Functional couplings between DMN and cerebral networks within these patterns were then calculated. Subsequently, associations between DMN subsystem couplings and behaviors were assessed, and lasso regression was used to evaluate their predictive effects on behavior. Moderation analyses and cytokine-based subgroup comparisons were further conducted to examine the effect of inflammation on brain-behavior relationships.

**Results:** In MDD, couplings within the DMN increased, whereas couplings between DMN and attention and salience networks decreased. Additionally, the association was observed between DMN B coupling and Trail Making Test Part B (TMT-B) performance in MDD. These alterations also predicted the digital span test (DST).

Moderation analyses showed that interleukin (IL)-17A strengthened DMN-behavior associations, whereas IL-8 attenuated them. Consistently, higher IL-17A levels were associated with more pronounced DMN coupling abnormalities, while lower IL-8 levels were linked to DST and TMT-B deficits.

**Conclusions:** This study demonstrates internal enhancement and external decoupling of the DMN in MDD, along with the differential modulation of inflammation on brain-behavior relationships. These findings provide new insights into the pathophysiology of MDD.

**Trial registration:** not applicable.

**Keywords:** Major depressive disorder, Default mode network, Periodic spatiotemporal patterns, Functional coupling, Inflammation.

## 1 Introduction

Major depressive disorder (MDD) has been recognized as one of the most prevalent psychiatric disorders worldwide [1, 2], typically characterized by persistent depressive mood, anhedonia, and recurrent suicidal ideation [3]. Patients with MDD exhibit impairments across multiple neuropsychological domains, including alexithymia [4], attentional deficits [5], and executive dysfunction [6, 7]. Although progress has been made in elucidating neural mechanisms and developing antidepressant treatments, the core pathophysiological mechanisms underlying MDD and its associated behavioral dysfunctions remain poorly understood.

Functional magnetic resonance imaging (fMRI) has become a pivotal modality for investigating the neurobiological mechanisms of MDD [8, 9]. Extensive evidence highlights that the default mode network (DMN) plays a central role in the pathophysiology of MDD [10-12]. Studies have found that patients with MDD often exhibit DMN hyperactivity [13, 14], which is associated with lifetime depression risk and maladaptive internally focused thinking such as rumination. Moreover, reduced connectivity between the DMN and visual, sensorimotor, and attention networks may be related to psychomotor retardation and cognitive impairment [15, 16]. Importantly, the DMN consists of three subsystems, including the

core, the dorsal medial, and the medial temporal subsystems, which are involved in functions such as information integration, social cognition, and episodic memory, respectively [17, 18]. Accumulating evidence indicates that the core and dorsal DMN subsystems are critically involved in maladaptive rumination in patients with MDD [19-22]. Moreover, increased connectivity within the dorsal DMN is associated with greater depressive symptom severity [23]. These findings highlight aberrant DMN connectivity as a critical neural target for understanding the pathophysiology of MDD.

Furthermore, most existing studies have focused on static functional connectivity, with less attention to the dynamic evolution of DMN interactions. Brain function exhibits intrinsic spatiotemporal dynamics, and network interactions fluctuate with ongoing internal states [24]. Disruptions in these dynamics, such as reduced flexibility or impaired stability, may constitute an important neural mechanism of depression [25, 26]. Recent evidence indicates reduced temporal variability of the DMN in MDD, which relates to negative self-focused thinking [27]. MDD subtypes with distinct DMN features have also been identified via dynamic analyses [28]. Nevertheless, the rhythmic reconfiguration of brain networks across spatiotemporal scales remains poorly explored. Periodic spatiotemporal patterns reflect slow rhythmic activity between the

DMN and the task-positive network (TPN) and are considered an important feature of intrinsic brain dynamics [29]. To date, PSTP has not been systematically investigated in MDD. This study of PSTPs in MDD holds promise for elucidating impairments in large-scale network coordination and providing novel insights into the core neurodynamic mechanisms of depression.

MDD involves a complex pathophysiology that cannot be fully explained by neuroimaging evidence alone. The inflammation hypothesis proposes that abnormal immune activation and neuroinflammation are important mechanisms underlying the onset and maintenance of depression. Meta-analyses have reported elevated levels of inflammatory markers, including interleukin (IL)-6, high-sensitivity C-reactive protein (hs-CRP), and IL-17A in MDD [30-32]. Among these, IL-17A is a key pro-inflammatory cytokine that contributes to abnormalities in depression related neural circuits by enhancing neuroinflammatory responses, influencing blood-brain barrier permeability and synaptic function [33]. Elevated levels of IL-17A are associated with increased severity of depressive symptoms [34, 35]. In addition, IL-8 has attracted increasing attention due to its dual roles in immune activation and regulation of neuroplasticity. It has been proposed as a potential biomarker for treatment-resistant depression [36] and is associated with altered brain

function and cognitive performance in patients with MDD [37, 38]. However, the relationships among inflammatory levels, dynamic brain network activity, and behavioral impairments remain unclear. Based on these findings, the present study hypothesizes that inflammatory cytokines may influence emotional and cognitive functions in depression by modulating the dynamic activity of large-scale neural circuits, providing a theoretical framework for investigating inflammation–brain network–behavior relationships.

This study aimed to characterize the PSTP in MDD and to examine functional couplings between distinct DMN subsystems and other large-scale brain networks within these patterns. To elucidate the relationships between DMN subsystems and behavioral measures in MDD, these couplings were first correlated with behaviors and subsequently used to predict behaviors. Furthermore, moderation analyses were conducted to assess the influence of inflammatory factors on brain–behavior relationships. Considering individual differences in inflammation and the existence of potential inflammatory subgroups, functional and behavioral differences were further explored across subgroups stratified by inflammatory cytokines. By integrating multidimensional data on brain networks, behavior, and inflammation, the study provides novel insights into the core pathophysiology of MDD.

## **2 Materials and Methods**

### **2.1 Participants**

Patients with depression were recruited from the Clinical Hospital of Chengdu Brain Science Institute between March 2023 and May 2024. All patients were diagnosed by specialized psychiatrists according to the Diagnostic and Statistical Manual of Mental Disorders, Fifth Edition, Text Revision (DSM-5) [39]. Participants were included in this study if they met the following criteria: (1) meeting the DSM-5 diagnostic criteria for MDD; (2) a 17-item Hamilton Depression Rating Scale (HAMD-17) total score > 17; (3) right-handedness; (4) ethnicity Han Chinese; (5) aged 16 years or older; (6) at least primary school education; and (7) willingness to participate in the study and to receive treatment. Exclusion criteria included neurological or severe medical disorders, substance abuse or dependence, comorbid psychiatric disorders, pregnancy or lactation, recent neuromodulation treatments (within 6 months), implanted metal or electronic devices, and any contraindications to MRI or neuropsychological assessment. Based on these criteria, 87 patients with MDD (age =  $26.10 \pm 7.43$  years, 70 females) were included in the present study.

To provide a neuroimaging reference, 104 demographically

matched healthy control subjects (age =  $27.09 \pm 9.88$  years, 74 females) were also recruited as the healthy control (HC) group. All HCs included in this study met the following criteria: (1) right-handedness; (2) Han Chinese ethnicity; (3) aged 16 years or older; (4) at least primary school education; (5) no history of psychiatric or neurological disorders; (6) no family history of psychiatric disorders; (7) no history of major medical comorbidities, including autoimmune diseases, chronic inflammatory diseases, or endocrine disorders (e.g., thyroid disease, diabetes); (8) no acute infection or inflammatory symptoms and no use of medications that could affect immune or inflammatory status within the two weeks before participation; (9) no history of alcohol or drug abuse; and (10) no contraindications to MRI.

Written informed consent was obtained from all subjects (or their legal guardians if they were under 18 years old). All study methods and procedures were approved by the Research Ethics Committee of Chengdu Mental Health Center (approval number: CDMHLL-2017008), in accordance with the Declaration of Helsinki.

## **2.2 Clinical Behavioral Assessments**

A total of seven behavioral and clinical assessments were administered, all evaluated by a clinical psychologist. Depressive symptom was assessed using the HAMD-17 [40], and anxiety

symptoms were measured with the Hamilton Anxiety Rating Scale (HAMA) [41]. Emotional traits were evaluated using the Snaith-Hamilton Pleasure Scale (SHAPS) to assess anhedonia [42]. Cognitive function was examined using the Digit Span Test (DST) [43] and the Trail Making Test (TMT-A and TMT-B) [44], which capture working memory capacity and executive control efficiency. In addition, subjective cognitive deficits were assessed using the Perceived Deficits Questionnaire-Depression (PDQ-D) [45]. These scales collectively captured core symptom dimensions of MDD, including affective, emotional processing, and cognitive performance domains.

### **2.3 Image Data Acquisition**

MRI data were acquired using a SIEMENS 3T scanner. All participants were given foam padding to reduce head motion. The fMRI images were collected using an echo-planar imaging sequence. The following scanning parameters were used: slices = 34; TR/TE = 2000 ms/30 ms; flip angle = 90°; FOV = 240 × 240 mm<sup>2</sup>; matrix size = 64 × 64, and thickness = 4.4 mm and 255 volumes in each run. Axial anatomical T1-weighted images were attained using a 3-dimensional fast spoiled gradient echo (T1-3D FSPGR) sequence: TR = 2300 ms, TE = 2.32 ms, FA = 8°, matrix size = 256 × 256, FOV = 256 × 256 mm<sup>2</sup>, slice thickness = 0.9 mm, 192 slices without a gap.

During scanning, the subjects were instructed to keep their eyes closed and not to fall asleep.

## **2.4 Data Preprocessing**

The preprocessing procedures followed the approach described in the previous work [29], including discarding the first five time points, estimating head motion, performing slice-timing correction, and aligning functional images to the individual T1-weighted anatomical image using boundary-based registration. Additional processing steps were implemented. (1) Physiological and non-neuronal noise sources were further controlled by regressing out head motion (Friston-24 head-motion parameters), white matter, and cerebrospinal fluid signals, as well as the global signal. (2) Temporal filtering was conducted using a band-pass range of 0.01-0.1 Hz. (3) Cortical data were then reduced to  $N$  parcels (where  $N$  is the dimension of the parcellation), and the resulting parcel-wise time series were standardized to have zero mean and unit variance. Cortical parcellation was carried out using a multimodal brain atlas that divides the cortex into 360 parcels ( $N = 360$ ) [46].

## **2.5 Measurement of Inflammatory Cytokine Levels**

Fasting peripheral venous blood samples were collected from participants between 7:00 and 9:00 a.m. Serum cytokine levels were quantified using flow cytometry in combination with the Cytometric

Bead Array Human Th1/Th2/Th17 Kit (BD Biosciences), including IL-1 $\beta$ , IL-2, IL-4, IL-5, IL-6, IL-8, IL-10, IL-12p70, IL-17A, interferon- $\alpha$  (IFN- $\alpha$ ), interferon- $\gamma$  (IFN- $\gamma$ ), tumor necrosis factor- $\alpha$  (TNF- $\alpha$ ), and tumor necrosis factor- $\beta$  (TNF- $\beta$ ). In addition, high-sensitivity C-reactive protein (hs-CRP), a sensitive marker of low-grade systemic inflammation, was measured using a high-sensitivity immunoturbidimetric assay.

## **2.6 Periodic Spatiotemporal Pattern and Coupling**

### **Analysis**

#### **2.6.1 Individual-Tailored PSTP Detection**

The PSTP detection algorithm used in this study, adapted from our previous work [29], identifies dynamic, repeating patterns of brain functional networks over time. To obtain a robust and individual-tailored PSTP, four procedures were implemented. (1) A window (window length = 10TR) was randomly selected as an initial template. The template was then correlated with all sliding windows across the time series, and those with high similarity were averaged to update the template. This iterative process was repeated until convergence, resulting in a set of repeated spatiotemporal patterns (RSTPs). (2) From these RSTPs, a representative repeated pattern (RRP) was selected to capture the anti-correlated transition between DMN and TPN. In brief, the RRP is characterized by an initial

decrease in DMN activity as TPN activity rises, followed by an inversion of these dynamics (Fig. 1A). The DMN and TPN masks were derived from pre-established group-level masks (see Supplementary Material). (3) The period length of the RRP was defined as the number of time points between the start and end points of minimal difference in the fitted DMN and TPN signals (as shown in Figure S1). (4) This period length was used as the new window length, and procedures (1) - (3) were repeated iteratively until the period length stabilized. The RRP and period length of RRP obtained from the last iteration were defined as a robust individual-tailored PSTP and period length of the individual-tailored PSTP, respectively. To further characterize the spatiotemporal features of the PSTP, three metrics were calculated, including strength, frequency, and interval time. Further algorithmic details are provided in the Supplementary Materials.

### **2.6.2 Functional Coupling of the DMN within PSTP**

Following a previous study [47],  $N$  cortical regions were parcellated into 17 networks. Within this framework, DMN A represents the core subsystem, DMN B represents the dorsal medial subsystem, and DMN C represents the medial temporal subsystem (Supplementary Figure S2). Specifically, the core subsystem (DMN A) comprises the anterior medial prefrontal cortex

and the posterior cingulate cortex; the dorsal medial subsystem (DMN B) is anchored in the dorsal medial prefrontal cortex, lateral temporal cortex, temporal pole, and temporoparietal junction; and the medial temporal subsystem (DMN C) involves the inferior parietal lobule, retrosplenial cortex, and hippocampal formation.

To characterize the spatiotemporal coupling of distinct DMN subsystems, the time series of parcels within each DMN subsystem defined in the PSTP were correlated with those of all cortical parcels using Spearman correlation. The resulting correlation coefficients were then transformed using the Fisher  $r$ -to- $z$  algorithm to approximate a normal distribution for subsequent statistical analyses.

## **2.7 Correlation Analysis between DMN Functional Coupling and Behaviors**

To characterize the associations between functional coupling of DMN subsystems and behavioral abnormalities in MDD, partial correlation analyses were conducted between functional coupling and behavioral measures, with age, sex, head motion, and years of education included as covariates.

## **2.8 Behavioral Prediction Based on DMN Functional Coupling**

LASSO regression was employed to predict behavioral scores

using DMN functional couplings that showed significant differences between the MDD and HC groups as predictors (Fig. 1B). To prevent overfitting and ensure unbiased performance estimation, a nested cross-validation framework was implemented.

Specifically, an outer 10-fold cross-validation loop was used to partition the data into training and test sets. In each outer fold, 90% of the data served as the training set and the remaining 10% as the test set. Within each outer training set, an inner 10-fold cross-validation was performed to select the optimal regularization parameter  $\lambda$ . The  $\lambda$  that minimized the mean squared error across the inner folds was chosen. The model was then refitted on the entire outer training set using that  $\lambda$  and evaluated on the outer test set. This process was repeated across all outer folds, yielding a predicted value for every participant. The overall model performance was assessed by computing the Pearson correlation between these predicted values and the observed behavioral scores across all participants.

To prevent overfitting and perform variable selection simultaneously, the regularization parameter was optimized via 10-fold cross-validation. To evaluate the statistical significance of the predictive performance, a permutation test was conducted (1,000 permutations,  $p < 0.05$ ). In each permutation, a set of edges equal

in number to the coupling differences was randomly drawn from all available couplings, and the entire modeling and prediction procedure was repeated.

## **2.9 Moderation Analysis of Inflammatory Cytokines on DMN Functional Coupling and Behavior**

To investigate whether inflammatory cytokines modulate the association between DMN functional coupling and behavioral performance, a moderation analysis was performed (Fig. 1C). In the model, DMN functional coupling was treated as the dependent variable, behavioral scores as the independent variable, and inflammatory cytokines as the moderator.

## **2.10 Subgroup Classification of MDD Based on Inflammatory Cytokines**

To further investigate how different levels of inflammatory cytokines affect behavioral performance, PSTP spatiotemporal characteristics, and DMN functional coupling, subgroup analyses were conducted for each inflammatory cytokine that exhibited a significant moderation effect (Fig. 1D). Specifically, for each such cytokine, patients with MDD were stratified into high- and low-inflammation subgroups according to the mean cytokine levels within the MDD group, resulting in a distinct subgroup structure for each cytokine. Subsequently, differences in behavioral measures

and neuroimaging indices were compared among these subgroups and the HC group, and the associations between these measures and behaviors were examined within each subgroup.

## **2.11 Statistical Analysis**

Statistical analyses were performed using SPSS Statistics 26.0 and MATLAB. Categorical variables were compared using the Chi-square test. The normality of continuous variables was assessed using the Kolmogorov-Smirnov test. For variables following a normal distribution, group differences were evaluated using two-tailed independent-samples *t*-tests. If not normally distributed, the Mann-Whitney *U* test was applied. Differences in behavioral and neuroimaging measures among the MDD subgroups and the HC group were assessed using the Kruskal-Wallis test, followed by Dunn's post-hoc test. Multiple comparisons were corrected using the Bonferroni method (corrected  $p < 0.05$ ). Age, sex, and years of education were controlled for in the behavioral and inflammatory cytokine analyses. In the imaging analyses, head motion was additionally included as a covariate. Given the limited sample size in subgroup analyses, this study reports effect sizes for non-parametric tests [48] and confidence intervals for correlation analyses.

## **3 Results**

### **3.1 Demographic Information and Clinical**

## Characteristics

Robust individual-tailored PSTPs were successfully identified in 85 HCs and 74 MDD patients. For subsequent analyses, only participants in whom individual-tailored PSTPs were successfully identified were included. The demographic characteristics, behavioral performance, and inflammatory cytokine levels of these participants are summarized in Table 1. No significant differences were observed between the MDD and HC groups in the demographic characteristics. Furthermore, all behavioral measures in the MDD group were significantly higher than those in the HC group, except for the DST score, which was significantly lower in MDD (independent-samples  $t$ -test,  $p < 0.05$ ). Regarding inflammatory cytokines, significantly increased serum IL-5 and IL-10 levels were observed in MDD compared with HC, whereas significantly decreased IL-8 levels were observed (Mann-Whitney U test,  $p < 0.05$ ). No significant differences were observed for the remaining cytokines. Note that the number of subjects included in each inflammatory cytokine may vary (see Supplementary Materials for details).

### 3.2 Individual-tailored PSTP

DMN and TPN masks were generated by locating areas strongly correlated or anti-correlated with the posterior cingulate cortex,

respectively (Supplementary Figure S3). Each subject exhibited unique period lengths (Supplementary Figure S4), with a median duration of 20 seconds (10 timepoints).

The individual-tailored PSTPs demonstrated anti-correlated transitions between the DMN and TPN, with an example shown in Supplementary Figure S5. To assess potential disruptions of the PSTP in MDD, this study quantified the features of PSTP and performed group comparisons using the nonparametric Mann-Whitney  $U$  test. However, no significant group differences were observed in the strength, frequency, or interval time of the PSTP, nor in the period length between the MDD and HC groups.

### **3.3 Analysis of DMN Functional Coupling Based on PSTP**

To characterize the temporal features of the DMN within the PSTP, couplings were estimated between each DMN subsystem and all cortical regions using Spearman correlation. Compared with HC, patients with MDD exhibited significant alterations in 12 functional couplings (independent-samples  $t$ -test,  $p < 0.001$ ). Specifically, MDD showed decreased coupling of the DMN A subsystem with the ventral attention network (VAN) (L\_23d - R\_23c and L\_31a - R\_5mv), salience network (SN) (R\_31a - R\_a32pr), and visual peripheral network (R\_10d - R\_V3CD), but increased coupling with Control B

(R\_s32 - R\_i6-8). The DMN B subsystem showed decreased coupling with the dorsal attention network A (DAN A) (R\_45 - L\_PGp) and increased coupling with the temporo-parietal junction (TPJ) (R\_47m - R\_STGa), while the DMN C subsystem demonstrated decreased coupling with the ventral attention network (VAN) (R\_POS1 - R\_FOP4 and R\_POS1 - R\_FOP3) and SN (R\_H - L\_FOP5). Within-DMN coupling was generally enhanced, particularly between the DMN A and DMN C subsystems (R\_10r - R\_H and L\_v23ab - R\_H). To improve readability, each parcel-level edge was accompanied in Table 2 by its corresponding functional brain region based on established network assignments. Detailed results are presented in Fig. 2 and Table 2.

### **3.4 Correlation between Coupling Differences and Behaviors**

In patients with MDD, a significant negative correlation was found between TMT-B scores and the functional coupling of R\_45 - L\_PGp ( $r = -0.31$ ,  $p = 0.010$ ) (Fig. 3).

### **3.5 Behavioral Prediction Based on Coupling Differences**

The significantly altered functional couplings were selected as predictors in a LASSO regression model to predict the behavioral manifestation of MDD. The model retained 8 edges for predicting

DST scores (Fig. 4). Among these, the DMN C - SN (R\_H - L\_FOP5) and DMN A - VAN (L\_23d - R\_23c) couplings showed the largest contributions. The correlation between the predicted and observed DST scores was  $r = 0.53$  ( $p < 0.001$ ), and the permutation test further confirmed the significance of this predictive relationship ( $p = 0.029$ ), indicating robust model performance.

### **3.6 Moderation Analysis of Inflammatory Cytokines on DMN Functional Coupling and Behavior**

To examine whether the relationship between DMN functional coupling and behaviors was influenced by inflammatory cytokines, moderation analyses were conducted. Three significant moderation effects were identified in the MDD group (Fig. 5 and Table 3). Specifically, IL-8 positively moderated the negative association between the L\_PGp - R\_45 coupling and TMT-B scores, whereas IL-17A negatively moderated the association between the same coupling and TMT-B scores.

### **3.7 Subgroup Analysis Based on Inflammatory Cytokines**

Moderation analysis revealed that inflammatory cytokines modulate the association between DMN coupling and behavioral measures. To further verify the impact of inflammation levels on brain function and behavior, this study classified patients with MDD

into high- and low-inflammation subgroups according to the cytokines showing significant moderating effects (IL-8 and IL-17A), and compared behavioral and imaging differences under different levels.

### **3.7.1 Subgroup Analysis Based on IL-8**

Using the mean of IL-8 levels as the cutoff, patients with MDD were divided into a high-inflammation group (Number of subjects:  $n = 14$ ) and a low-inflammation group ( $n = 48$ ). Eight functional couplings showed significant group differences (Kruskal-Wallis test,  $p < 0.001$ ) (Supplementary Table S1). The current study focused on the 12 DMN functional couplings previously identified as significant. Post-hoc analysis (Dunn test with Bonferroni correction,  $p < 0.05$ ) showed that R\_31a - R\_a32pr coupling was reduced in the high-inflammation group compared with HC, while no difference was observed in the low-inflammation group (Fig. 6A). For behaviors, several measures differed across groups (Kruskal-Wallis test,  $p < 0.05$ ) (Supplementary Table S2). This study focused on measures showing subgroup-specific patterns. Decreased DST and increased TMT-B scores were observed in the low-inflammation group compared with HC, whereas no significant differences were found between the high-inflammation group and HC, or between the two inflammation subgroups (Dunn test with Bonferroni correction,  $p <$

0.05) (Fig. 6B and 6C). Regarding inflammatory cytokines, higher IL-8 levels were observed in the high-inflammation group than in both the low-inflammation group and HC, whereas lower IL-8 levels were observed in the low-inflammation group compared with HC (Supplementary Table S2).

### **3.7.2 Subgroup Analysis Based on IL-17A**

Similarly, using the mean of IL-17A levels as the cutoff, patients with MDD were divided into a high-inflammation group ( $n = 22$ ) and a low-inflammation group ( $n = 41$ ). In the high-inflammation group, R\_47m - R\_STGa coupling was increased relative to HC, whereas R\_45 - L\_PGp coupling was decreased. Moreover, in the low-inflammation group, L\_31a - R\_a32pr coupling was decreased compared with HC (Fig. 6D and Supplementary Table S3). For behavioral performance, both inflammation subgroups differed from HC, but no subgroup-specific behavioral patterns were observed (Supplementary Table S4). Regarding inflammatory cytokines, the high-inflammation group showed increased IL-17A levels compared with the low-inflammation group, with no significant difference relative to HC, and exhibited decreased IL-6 levels relative to the low-inflammation group. Both inflammation subgroups showed lower IL-8 levels relative to HC (Supplementary Table S4). Notably, in the high-inflammation group, R\_47m - R\_STGa coupling was

positively correlated with TMT-B scores ( $r_{\text{Spearman}} = 0.59$ ,  $p = 0.006$ , 95% CI: [0.20, 0.81]) (Fig. 6E).

## 4 Discussion

This study characterized aberrant functional couplings of the DMN in MDD using PSTP and explored their associations with behavior and inflammation. Specifically, patients with MDD exhibited increased within-DMN coupling and decreased coupling with external networks, reflecting an “internal enhancement and external decoupling” pattern. Further correlation and predictive analyses revealed that associations between DMN subsystems and specific dimensions of cognitive impairment in MDD. Importantly, the relationship between DMN coupling and behavior in MDD was differentially modulated by IL-17A and IL-8. Subgroup analyses further supported this differential modulation. Overall, this study integrates multidimensional information across brain networks, behavior, and inflammation, demonstrating that neural dynamic dysregulation and specific inflammatory pathways jointly shape core pathological features of MDD, offering a new framework for understanding its pathophysiology.

This study differs from conventional dynamic connectivity analyses, which typically characterize time-varying fluctuations of

connectivity directly from the preprocessed time series and primarily focus on average connectivity strength or short-term dynamic changes [49, 50]. However, such methods are susceptible to sliding-window averaging effects and may fail to capture the higher-order temporal organization of network interactions [51]. In contrast, the present study first extracted PSTP based on the intrinsic anti-correlated rhythm between the DMN and TPN, and then characterized network reconfiguration within this dynamic framework. This approach enabled the identification of abnormalities in large-scale network coordination that are difficult to detect using traditional dynamic connectivity methods [29]. The results showed that although the overall periodic properties (e.g., period length) were comparable between MDD and HC, patients with MDD exhibited impaired network coordination during periodic reconfiguration. A previous study also suggested that DMN connectivity abnormalities in MDD are closely linked to the quasi-periodic neural activity [52]. These findings indicate that the core alteration in MDD may not be the absence of rhythmicity, but rather in disrupted transitions and integration between functional networks. Such impaired dynamical coordination may further lead to an imbalance between internally directed thought and external cue processing, promoting ruminative thinking and emotional

processing biases.

The current study confirms that MDD patients exhibited internal enhancement and external decoupling during periodic reconfiguration, indicating a shift of information processing from external to internal focus. A recent multicenter study reported that both the DMN activation and the DMN-attention network deactivation states were temporally unstable in MDD, with more frequent state transitions, suggesting that highly variable DMN fluctuations may amplify internal self-referential thinking and heighten sensitivity to rumination and emotional stimuli [53]. Meanwhile, reduced DMN-attention coupling may also underlie attentional deficits [54, 55]. Additionally, enhanced DMN-Control B coupling may reflect compensation. A prior study has shown that increased DMN-control network connectivity in MDD may serve to maintain cognitive function [56]. Other studies have observed hyperactivation of executive control networks during working memory or executive tasks in the absence of behavioral deficit [57, 58]. Thus, the present study speculates that increased DMN-control network coupling may represent an adaptive response aimed at preserving normative cognitive behavior in MDD, though further research is needed to confirm this interpretation. These results reveal disrupted DMN coordination and potential compensatory

mechanisms during periodic reconfiguration in MDD, providing a neural basis for emotional and cognitive impairments.

Moreover, the correlation between DMN B-DAN A coupling and TMT-B scores suggests that impaired dynamic switching between large-scale networks occurs during cognitive shifting tasks in MDD. As a classic executive function test, TMT-B primarily assesses cognitive flexibility and mental shifting ability [43]. This process relies on efficient switching between the DMN and DAN [59, 60]. Therefore, the abnormal DMN-DAN coupling characterized in the PSTP may represent an important neural mechanism underlying executive dysfunction in MDD. In contrast, TMT-A focuses more on basic processing speed and visual search [61] and depends less on cross-network dynamic regulation. Furthermore, PDQ-D, as a subjective cognitive measure, is influenced by emotional states and primarily reflects emotion-cognition interactions. Previous research has reported a complex relationship between DMN and PDQ-D, without stable mediation effects [62]. Notably, although DST was not significantly correlated with DMN coupling, predictive analysis indicated a potential contribution of the medial temporal DMN. These inferences warrant further validation in future studies with more rigorous designs. Overall, these findings indicate that different DMN subsystems may influence cognitive domains through distinct

mechanisms.

From the perspective of the inflammatory hypothesis, this study revealed that the relationship between brain function and behavior was specifically modulated by inflammatory cytokines, suggesting that distinct inflammatory cytokines play divergent roles in the pathological progression of depression. Specifically, the negative modulation of IL-17A may amplify the detrimental impact of aberrant connectivity on cognitive processing. Previous studies support this view, showing that elevated IL-17A is associated with greater depression severity [63-65]. IL-17A can cross the blood-brain barrier, induce neuroinflammation and neurotoxicity [66], and impair cognitive regulatory function [67]. The current inflammatory subgroup analysis further supports this finding. The high IL-17A subgroup exhibited more pronounced coupling abnormalities, which were positively correlated with executive dysfunction (TMT-B scores). Additionally, IL-17A has been associated with antidepressant treatment response [68-70], suggesting that it may serve as a critical hub linking immune status, neural network alterations, and depression-related clinical phenotypes. Future longitudinal or interventional studies are warranted to clarify the causal role of IL-17A in network reconfiguration and to provide more direct evidence for inflammation-targeted therapeutic strategies.

Moreover, the positive modulatory effect of IL-8 suggests that, within a certain physiological range, IL-8 may enhance the facilitative effect of DMN coupling on cognitive performance. Subgroup analyses further support this notion, indicating a potential compensatory role of IL-8 in cognitive deficits in MDD. Previous studies have shown that IL-8 can exert both pro- and anti-inflammatory properties depending on the cellular environment [71]. Heterogeneous results have also been reported in studies related to MDD [72, 73], which may be related to differences in sample size, demographic characteristics, and medication status [74, 75]. The present findings further suggest that the underlying mechanisms of the heterogeneity may also be closely linked to ongoing brain network dynamics. Given the cross-sectional design of this study, future research should incorporate longitudinal tracking to further elucidate the complex relationships among peripheral inflammation, dynamic brain networks, and behavioral outcomes. Together, the differential moderation of the brain-behavior relationship by IL-8 and IL-17A underscores the heterogeneity of inflammatory effects in MDD. These results not only support the inflammatory hypothesis of depression but also highlight inflammatory subtyping as a promising direction for precision diagnosis and intervention.

## **Limitation**

There are several limitations to this study. First, the sample size was relatively small, which may limit statistical power and the generalizability of the finding. Future studies should include larger and more diverse cohorts, encompassing different MDD subtypes and illness stages. Second, the proportion of male participants in the MDD group was relatively low, which may have influenced the findings. Future studies should include samples with a more balanced sex distribution to systematically investigate the potential impact of sex on PSTP and the associated brain-behavior relationships. Third, the potential influence of acute stress on peripheral inflammatory levels could not be entirely excluded. Fourth, the cohort was not restricted to drug-naïve, first-episode MDD patients, and medications such as antidepressants, antipsychotics, or mood stabilizers may have affected cytokine levels. Future studies should control for medication type and cumulative dose and prioritize drug-naïve, first-episode patients. Additionally, confounding factors such as body mass index and lifestyle were not accounted for. Finally, the cross-sectional nature of this study precludes causal inference regarding the relationships between inflammation, functional coupling, and behavioral performance. Longitudinal designs are necessary to clarify the directionality and

causal precedence of these relationships.

## **5 Conclusion**

This study leveraged PSTP to reveal spatiotemporal functional dysregulation of the DMN underlying emotional and cognitive impairments in MDD. The current study further demonstrated that inflammatory cytokines differentially modulate the relationships between brain and behavior, suggesting that inflammation may influence emotional and cognitive function through distinct neural pathways. These findings support the inflammation hypothesis and indicate that the pathophysiology of MDD arises from the interplay between neural dynamics and inflammatory signaling. Together, this work provides a novel spatiotemporal network-inflammation framework for understanding the pathological basis of behavioral deficits in MDD.

**The abbreviation list:**

MDD = major depressive disorder;

HC = the healthy control;

fMRI = functional magnetic resonance imaging;

PSTP = periodic spatiotemporal pattern;

RSTP = repeated spatiotemporal pattern;

RRP = representative repeated pattern;

DMN = default mode network;

TPN = task-positive network;

SN = salience network;

VAN = ventral attention network;

HAMD-17 = 17-item hamilton depression rating scale;

HAMA = hamilton anxiety rating scale;

DST = digit span test;

TMT = trail making test;

PDQ-D = perceived deficits questionnaire-depression;

SHAPS = snaith-hamilton pleasure scale;

IL = interleukin;

hs-CRP = high-sensitivity C-reactive protein;

IFN- $\alpha$  = interferon- $\alpha$ ;

IFN- $\gamma$  = interferon- $\gamma$ ;

TNF- $\alpha$  = tumor necrosis factor- $\alpha$ ;

TNF- $\beta$  = tumor necrosis factor- $\beta$ ;

mFD = mean frame-wise displacement.

## **Ethics approval and consent to participate**

This study was approved by the Research Ethics Committee of Chengdu Mental Health Center (approval number: CDMHLL-2017008), in accordance with the Declaration of Helsinki. Written informed consent was obtained from all participants prior to their participation in the study (or their legal guardians if they were under 18 years old).

## **Consent for publication**

Not applicable.

## **Availability of data and materials**

The data that support the findings of this study are available on request from the corresponding author. The data are not publicly available due to privacy or ethical restrictions.

## **Competing interests**

The authors have no relevant financial or non-financial interests to disclose.

## **Funding**

This work was supported by National Key R&D Program of China, (2024YFE0215100), Brain Science and Brain-like Intelligence Technology- National Science and Technology Major Project (No. 2022ZD0208500), the National Nature Science Foundation of China (82371560, 62401124 and 62571106), the Natural Science Foundation of Sichuan (2023NSFSC0037), and the CAMS Innovation Fund for Medical Sciences (CIFMS) (No.2019-I2M-5-039).

## **Authors' contributions**

**Junxia Chen:** Writing - original draft, Software, Formal analysis, Data curation, Conceptualization. **Xiaoying Sun:** Project

administration, Data curation, Methodology, Investigation. **Suping Yue:** Conceptualization, Data curation, Funding acquisition, Investigation. **Zibin Feng:** Data curation, Software, Resources. **Ruikun Yang:** Methodology, Data analysis. **Yue Yu:** Writing - review & editing, Formal analysis. **Hui He:** Conceptualization, Project administration, Visualization. **Suli Zhao:** Data curation, Methodology. **Yifan Li:** Formal analysis. **Shuxiao Chen:** Software, Resources. **Roberto Rodriguez-Labrada:** Draft Revising - review & editing. **Mingjun Duan:** Investigation, Data curation. **Dezhong Yao:** Formal analysis, Funding acquisition, Project administration. **Sisi Jiang:** Conceptualization, Writing - review & editing. **Cheng Luo:** Draft Writing - review & revising, Conceptualization, Funding acquisition, Supervision, Resources, Project administration.

### **Acknowledgement**

We thank all the subjects who participated in this study. We thank all researchers and scientific advisors for their contribution to the design of this study. We thank our colleagues for their role in data collection. We also acknowledge the support from the China Scholarship Council.

### **Appendix. Supplementary materials**

Supplementary Material.

## References

1. Berk, M., O. Köhler-Forsberg, M. Turner, B.W.J.H. Penninx, A. Wrobel, J. Firth, et al., *Comorbidity between major depressive disorder and physical diseases: a comprehensive review of epidemiology, mechanisms and management*. World Psychiatry, 2023. **22**(3): p. 366-387.
2. Kautzky, A., G. James, C. Philippe, P. Baldinger-Melich, C. Kraus, G. Kranz, et al., *The influence of the rs6295 gene polymorphism on serotonin-1A receptor distribution investigated with PET in patients with major depression applying machine learning*. 2017. **7**(6): p. e1150-e1150.
3. Otte, C., S.M. Gold, B.W. Penninx, C.M. Pariante, A. Etkin, M. Fava, et al., *Major depressive disorder*. Nature Reviews Disease Primers, 2016. **2**.
4. Tian, Y.H., Y.G. Cui, L.W. Liu, C.H. Chen, Z.W. Liu, W.Z. Li, et al., *Depressive and mobile phone addiction symptoms in Chinese adolescents with major depressive disorder: the mediating effect of alexithymia*. BMC Psychiatry, 2025. **25**(1).
5. Garcia-Argibay, M., I. Brikell, A. Thapar, P. Lichtenstein, S. Lundstroem, D. Demontis, et al., *Attention-Deficit/Hyperactivity Disorder and Major Depressive Disorder: Evidence From Multiple Genetically Informed Designs*. Biological Psychiatry, 2024. **95**(5): p. 444-452.
6. Li, Y.T., C. Zhang, J.C. Han, Y.X. Shang, Z.H. Chen, G.B. Cui, et al., *Neuroimaging features of cognitive impairments in schizophrenia and major depressive disorder*. Therapeutic Advances in Psychopharmacology, 2024. **14**.
7. Sun, F.P., Z.N. Liu, J. Yang, Z.B. Fan, F.W. Wang and J. Yang, *Aberrant brain dynamics in major depressive disorder during working memory task*. European Archives of Psychiatry and Clinical Neuroscience, 2025. **275**(4): p. 1141-1150.
8. Hagen, J., S. Ramkiran, G.J. Schnellbaecher, R. Rajkumar, M. Collee, N. Khudeish, et al., *Phenomena of hypo- and hyperconnectivity in basal ganglia-thalamo-cortical circuits linked to major depression: a 7T fMRI study*. Molecular Psychiatry, 2025. **30**(1): p. 158-167.
9. Kochunov, P., B.M. Adhikari, D. Keator, D. Amen, S. Gao, N.R. Karcher, et al., *Functional vs Structural Cortical Deficit Pattern Biomarkers for Major Depressive Disorder*. Jama Psychiatry, 2025. **82**(6): p. 582-590.
10. Zhang, L., K. Qin, N. Pan, H. Xu and Q.J.J.o.A.D. Gong, *Shared and distinct patterns of default mode network dysfunction in major depressive disorder and bipolar disorder: A comparative meta-analysis*. 2025. **368**: p. 23-32.

11. Williams, L.M.J.D. and anxiety, *Defining biotypes for depression and anxiety based on large-scale circuit dysfunction: A theoretical review of the evidence and future directions for clinical translation*. 2017. **34**(1): p. 9-24.
12. Lu, F., J. Zhang, Y. Zhong, L. Hong, J. Wang, H. Du, et al., *Neural signatures of default mode network subsystems in first-episode, drug-naive patients with major depressive disorder after 6-week thought induction psychotherapy treatment*. 2024. **6**(4): p. fcae263.
13. Afriyie-Agyemang, Y., M.A. Bertocci, S. Iyengar, R.S. Stiffler, L.K. Bonar, H.A. Aslam, et al., *Lifetime depression and mania/hypomania risk predicted by neural markers in three independent young adult samples during working memory and emotional regulation*. *Molecular Psychiatry*, 2025. **30**(3): p. 870-880.
14. Tozzi, L., X. Zhang, A. Pines, A.M. Olmsted, E.S. Zhai, E.T. Anene, et al., *Personalized brain circuit scores identify clinically distinct biotypes in depression and anxiety*. *Nature Medicine*, 2024. **30**(7): p. 2076-2087.
15. Buyukdura, J.S., S.M. McClintock and P.E. Croarkin, *Psychomotor retardation in depression: Biological underpinnings, measurement, and treatment*. *Progress in Neuro-Psychopharmacology & Biological Psychiatry*, 2011. **35**(2): p. 395-409.
16. Javaheripour, N., M. Li, T. Chand, A. Krug, T. Kircher, U. Dannlowski, et al., *Altered resting-state functional connectome in major depressive disorder: a mega-analysis from the PsyMRI consortium*. *Translational Psychiatry*, 2021. **11**(1).
17. Smallwood, J., B.C. Bernhardt, R. Leech, D. Bzdok, E. Jefferies and D.S. Margulies, *The default mode network in cognition: a topographical perspective*. *Nature Reviews Neuroscience*, 2021. **22**(8): p. 503-513.
18. Satpute, A.B. and K.A. Lindquist, *The Default Mode Network's Role in Discrete Emotion*. *Trends in Cognitive Sciences*, 2019. **23**(10): p. 851-864.
19. Kim, J., J.R. Andrews-Hanna, H. Eisenbarth, B.K. Lux, H.J. Kim, E. Lee, et al., *A dorsomedial prefrontal cortex-based dynamic functional connectivity model of rumination*. *Nature Communications*, 2023. **14**(1).
20. Zhou, H.X., X. Chen, Y.Q. Shen, L. Li, N.X. Chen, Z.C. Zhu, et al., *Rumination and the default mode network: Meta-analysis of brain imaging studies and implications for depression*. *Neuroimage*, 2020. **206**.
21. Tozzi, L., X. Zhang, M. Chesnut, B. Holt-Gosselin, C.A. Ramirez and L.M. Williams, *Reduced functional connectivity of default mode network subsystems in depression: Meta-analytic evidence and relationship with trait rumination*. *Neuroimage-Clinical*, 2021. **30**.

22. Jia, F., X. Chen, X. Wang, C. Quan, J. Ruan, Y. Huang, et al., *Activity of the default mode network mediates the effect of peripheral plasma glial cell line-derived neurotrophic factor levels on rumination in major depressive disorder patients*. 2025. **5**: p. kkaf014.
23. Qiu, H., L.Q. Zhang, Y.X. Gao, Z.L. Zhou, H.L. Li, L.X. Cao, et al., *Functional connectivity of the default mode network in first-episode drug-naïve patients with major depressive disorder*. Journal of Affective Disorders, 2024. **361**: p. 489-496.
24. Zhang, J., W. Cheng, Z.W. Liu, K. Zhang, X. Lei, Y. Yao, et al., *Neural, electrophysiological and anatomical basis of brain-network variability and its characteristic changes in mental disorders*. Brain, 2016. **139**: p. 2307-2321.
25. Cheng, C., D.F. Dong, Y.L. Jiang, Q.S. Ming, X. Zhong, X.Q. Sun, et al., *State-Related Alterations of Spontaneous Neural Activity in Current and Remitted Depression Revealed by Resting-State fMRI*. Frontiers in Psychology, 2019. **10**.
26. Javaheripour, N., L. Colic, N. Opel, M. Li, S.M. Balajoo, T. Chand, et al., *Altered brain dynamic in major depressive disorder: state and trait features*. Translational Psychiatry, 2023. **13**(1).
27. Marchitelli, R., M.L. Paillère-Martinot, N. Bourvis, C. Guerin-Langlois, A. Kipman, C. Trichard, et al., *Dynamic Functional Connectivity in Adolescence-Onset Major Depression: Relationships With Severity and Symptom Dimensions*. Biological Psychiatry-Cognitive Neuroscience and Neuroimaging, 2022. **7**(4): p. 385-396.
28. Cai, A., J. Yang, H. Guo, S. Dong, T. Zhao, W. Zhou, et al., *Unraveling spatiotemporal dynamics in transdiagnosis subtypes of major depressive disorder and bipolar disorder: insights from co-activation patterns and treatment response*. 2025: p. 1-13.
29. Chen, J.X., S.S. Jiang, G.F. Ye, Z.H. Yang, C.Y. Hou, H.C. Li, et al., *Disrupted periodic spatiotemporal pattern and dynamic reorganization of its basic states in generalized epilepsy*. Journal of Neural Engineering, 2025. **22**(5).
30. Kim, I.B., J.H. Lee and S.C. Park, *The Relationship between Stress, Inflammation, and Depression*. Biomedicines, 2022. **10**(8).
31. Roohi, E., N. Jaafari and F. Hashemian, *On inflammatory hypothesis of depression: what is the role of IL-6 in the middle of the chaos?* Journal of Neuroinflammation, 2021. **18**(1).
32. Liu, J.J., Y.B. Wei, R. Strawbridge, Y.P. Bao, S.H. Chang, L. Shi, et al., *Peripheral cytokine levels and response to antidepressant treatment in depression: a systematic review and meta-analysis*. Molecular Psychiatry, 2020. **25**(2): p. 339-350.
33. Beurel, E., M. Toups and C.B. Nemeroff, *The Bidirectional Relationship of Depression and Inflammation: Double Trouble*.

- Neuron, 2020. **107**(2): p. 234-256.
34. Tsuboi, H., H. Sakakibara, Y. Minamida, H. Tsujiguchi, M. Matsunaga, A. Hara, et al., *Elevated Levels of Serum IL-17A in Community-Dwelling Women with Higher Depressive Symptoms*. Behav Sci (Basel), 2018. **8**(11).
  35. Tsuboi, H., H. Sakakibara, Y. Minamida-Urata, H. Tsujiguchi, A. Hara, K. Suzuki, et al., *Serum TNFalpha and IL-17A levels may predict increased depressive symptoms: findings from the Shika Study cohort project in Japan*. Biopsychosoc Med, 2024. **18**(1): p. 20.
  36. Szalach, L.P., K. Ciesielska-Figlon, A. Daca, W.J. Cubala and K.A. Lisowska, *The Effect of Ketamine on the Immune System in Patients with Treatment-Resistant Depression*. Int J Mol Sci, 2025. **26**(15).
  37. Shkundin, A. and A. Halaris, *IL-8 (CXCL8) Correlations with Psychoneuroimmunological Processes and Neuropsychiatric Conditions*. J Pers Med, 2024. **14**(5).
  38. Cai, Y., Z.H. Zhu, R.H. Li, X.Y. Yin, R.F. Chen, L.J. Man, et al., *Association between increased serum interleukin-8 levels and improved cognition in major depressive patients with SSRIs*. BMC Psychiatry, 2023. **23**(1): p. 122.
  39. Messent, P.J.C.c.p. and psychiatry, *DSM-5*. 2013. **18**(4): p. 479-482.
  40. Hamilton, M.J.J.o.n., neurosurgery, and psychiatry, *A rating scale for depression*. 1960. **23**(1): p. 56.
  41. Hamilton, M.J.B.j.o.m.p., *The assessment of anxiety states by rating*. 1959.
  42. Snaith, R.P., M. Hamilton, S. Morley, A. Humayan, D. Hargreaves and P.J.T.B.J.o.P. Trigwell, *A scale for the assessment of hedonic tone the Snaith-Hamilton Pleasure Scale*. 1995. **167**(1): p. 99-103.
  43. Wechsler, D., *Manual for the Wechsler adult intelligence scale*. 1955.
  44. Bowie, C.R. and P.D.J.N.p. Harvey, *Administration and interpretation of the Trail Making Test*. 2006. **1**(5): p. 2277-2281.
  45. Sullivan, M.J., K. Edgley and E.J.C.J.o.R. Dehoux, *A survey of multiple sclerosis: I. Perceived cognitive problems and compensatory strategy use*. 1990.
  46. Glasser, M.F., T.S. Coalson, E.C. Robinson, C.D. Hacker, J. Harwell, E. Yacoub, et al., *A multi-modal parcellation of human cerebral cortex*. Nature, 2016. **536**(7615): p. 171-178.
  47. Schaefer, A., R. Kong, E.M. Gordon, T.O. Laumann, X.N. Zuo, A.J. Holmes, et al., *Local-Global Parcellation of the Human Cerebral Cortex from Intrinsic Functional Connectivity MRI*. Cerebral Cortex, 2018. **28**(9): p. 3095-3114.
  48. Fiel Peres, F., *Effect sizes for nonparametric tests*. Biochem Med (Zagreb), 2026. **36**(1): p. 010101.
  49. Zhou, Y., Y.H. Zhu, H.T. Ye, W.H. Jiang, Y.B. Zhang, Y.Y. Kong, et al., *Abnormal changes of dynamic topological characteristics in patients*

- with major depressive disorder*. Journal of Affective Disorders, 2024. **345**: p. 349-357.
50. Yang, C.Y., Y.Y. Li, Y.T. Wang, H.L. Yang, Y.X. Ling, L. Wang, et al., *Sex-specific amygdala connectivity alterations in medication-naïve major depressive disorder: A static and dynamic analysis*. Progress in Neuro-Psychopharmacology & Biological Psychiatry, 2025. **142**.
  51. Vergara, V.M., A. Abrol and V.D. Calhoun, *An average sliding window correlation method for dynamic functional connectivity*. Human Brain Mapping, 2019. **40**(7): p. 2089-2103.
  52. Wang, K., W. Majeed, G. Thompson, K. Ying, Y. Zhu and S. Keilholz. *Quasi-periodic pattern of fMRI contributes to functional connectivity and explores differences between Major Depressive disorder and control*. in *Proc Int Soc Magn Reson Med*. 2016.
  53. An, Z.Q., K. Tang, Y.Y. Xie, C.J. Tong, J.M. Liu, Q. Tao, et al., *Aberrant resting-state co-activation network dynamics in major depressive disorder*. Translational Psychiatry, 2024. **14**(1).
  54. Tse, N.Y., A. Ratheesh, Y.E. Tian, C.G. Connolly, C.G. Davey, S. Ganesan, et al., *A mega-analysis of functional connectivity and network abnormalities in youth depression*. 2024. **2**(10): p. 1169-1182.
  55. Beckmann, F.E., H. Gruber, S. Seidenbecher, S.T. Schirmer, C.D. Metzger, L. Tozzi, et al., *Specific alterations of resting-state functional connectivity in the triple network related to comorbid anxiety in major depressive disorder*. 2024. **59**(7): p. 1819-1832.
  56. Wang, M., T. Chen, Z.Y. He, L.W.C. Chan, Q. Guo, S.Y. Cai, et al., *Altered dynamic functional connectivity in antagonistic state in first-episode, drug-naïve patients with major depressive disorder*. BMC Psychiatry, 2024. **24**(1).
  57. Williams, L.M., *Defining biotypes for depression and anxiety based on large-scale circuit dysfunction: a theoretical review of the evidence and future directions for clinical translation*. Depression and Anxiety, 2017. **34**(1): p. 9-24.
  58. Harvey, P.-O., P. Fossati, J.-B. Pochon, R. Levy, G. LeBastard, S. Lehericy, et al., *Cognitive control and brain resources in major depression: an fMRI study using the n-back task*. 2005. **26**(3): p. 860-869.
  59. Jacobson, S.C., M. Blanchard, C.C. Connolly, M. Cannon and H. Garavan, *An fMRI investigation of a novel analogue to the Trail-Making Test*. Brain Cogn, 2011. **77**(1): p. 60-70.
  60. Varjadic, A., D. Mantini, N. Demeyere and C.R. Gillebert, *Neural signatures of Trail Making Test performance: Evidence from lesion-mapping and neuroimaging studies*. Neuropsychologia, 2018. **115**: p. 78-87.
  61. Jiang, L., S.B. Eickhoff, S. Genon, G. Wang, C. Yi, R. He, et al.,

- Multimodal Covariance Network Reflects Individual Cognitive Flexibility*. Int J Neural Syst, 2024. **34**(4): p. 2450018.
62. Cui, Y., R. Lu, X. Liang, J. Li, H. Zhang, D. Li, et al., *Intrinsic Brain Activity Mediates the Relationship Between Depressive Symptoms and Subjective Cognitive Complaints in Young Adults in Higher Education: A Resting-State fMRI Study Based on Amplitude of Low-frequency Fluctuation*. Acad Radiol, 2025. **32**(10): p. 6158-6168.
  63. Tsuboi, H., H. Sakakibara, Y. Minamida, H. Tsujiguchi, M. Matsunaga, A. Hara, et al., *Elevated levels of serum IL-17A in community-dwelling women with higher depressive symptoms*. 2018. **8**(11): p. 102.
  64. Mao, L., X. Ren, X. Wang and F.J.J.o.i.r. Tian, *Associations between Autoimmunity and Depression: Serum IL-6 and IL-17 Have Directly Impact on the HAMD Scores in Patients with First-Episode Depressive Disorder*. 2022. **2022**(1): p. 6724881.
  65. Davami, M.H., R. Baharlou, A.A. Vasmehjani, A. Ghanizadeh, M. Keshtkar, I. Dezhkam, et al., *Elevated IL-17 and TGF- $\beta$  serum levels: a positive correlation between T-helper 17 cell-related pro-inflammatory responses with major depressive disorder*. 2016. **7**(2): p. 137.
  66. Kebir, H., K. Kreymborg, I. Ifergan, A. Dodelet-Devillers, R. Cayrol, M. Bernard, et al., *Human TH17 lymphocytes promote blood-brain barrier disruption and central nervous system inflammation*. 2007. **13**(10): p. 1173-1175.
  67. Brigas, H.C., M. Ribeiro, J.E. Coelho, R. Gomes, V. Gomez-Murcia, K. Carvalho, et al., *IL-17 triggers the onset of cognitive and synaptic deficits in early stages of Alzheimer's disease*. 2021. **36**(9).
  68. Bliźniewska-Kowalska, K., A. Halaris, P. Gałecki and M.J.J.o.A.D.R. Gałecka, *Role of interleukin 17 (IL-17) in the inflammatory hypothesis of depression*. 2023. **14**: p. 100610.
  69. Syed, S.A., E. Beurel, D.A. Loewenstein, J.A. Lowell, W.E. Craighead, B.W. Dunlop, et al., *Defective Inflammatory Pathways in Never-Treated Depressed Patients Are Associated with Poor Treatment Response*. Neuron, 2018. **99**(5): p. 914-+.
  70. Nava, R.G., A.S. Adri, I.S. Filgueiras, A.L. Nóbile, P.M. Barcelos, Y.L.G. Corrêa, et al., *Modulation of neuroimmune cytokine networks by antidepressants: implications in mood regulation*. 2025. **15**(1): p. 314.
  71. Matsushima, K., D. Yang and J.J. Oppenheim, *Interleukin-8: An evolving chemokine*. Cytokine, 2022. **153**: p. 155828.
  72. Kruse, J.L., M.M. Vasavada, R. Olmstead, G. Hellemann, B. Wade, E.C. Breen, et al., *Depression treatment response to ketamine: sex-specific role of interleukin-8, but not other inflammatory markers*. Transl Psychiatry, 2021. **11**(1): p. 167.

73. Kang, Y., D. Shin, A. Kim, W.S. Tae, B.J. Ham and K.M. Han, *Resting-state functional connectivity is correlated with peripheral inflammatory markers in patients with major depressive disorder and healthy controls*. J Affect Disord, 2025. **370**: p. 207-216.
74. Versel, J., A. Cantos, M.F.R. Castillo, E. Fatourou, J. Sinacore and A.J.J.o.A.D.R. Halaris, *Interleukin-8 is a potential inflammation biomarker in major depressive disorder*. 2024. **17**: p. 100828.
75. Cai, Y., Z.H. Zhu, R.H. Li, X.Y. Yin, R.F. Chen, L.J. Man, et al., *Association between increased serum interleukin-8 levels and improved cognition in major depressive patients with SSRIs*. 2023. **23**(1): p. 122.

**Table 1.** Demographic, behavioral, and inflammatory cytokine characteristics in the MDD and HC subjects with individual-tailored PSTPs.

<b>Characteristic</b>	<b>MDD</b>	<b>HC</b>	<b>Test</b>	<b>P value</b>
Number	74	85	-	-
Age (year)	26.61 (7.80)	27.49 (10.06)	-0.6	0.540 <sup>a</sup>
Sex (Male: Female)	13:61	26:59	3.62	0.057 <sup>b</sup>
Education (year)	14.96 (2.41)	15.62 (2.64)	-1.65	0.101 <sup>a</sup>
Illness Duration (year)	2.72 (4.88)	-	-	-
mFD (mm)	0.12 (0.06)	0.12 (0.04)	0.30	0.762 <sup>a</sup>
<b>Behavior</b>	-	-	-	-
HAMD	24.92 (4.74)	1.46 (1.72)	40.7 3	< 0.001 a*
HAMA	25.24 (8.34)	1.34 (1.53)	24.6 6	< 0.001 a*
SHAPS	32.47 (5.05)	22.05 (5.19)	9.62	< 0.001 a*
DST	11.18 (2.45)	12.98 (2.72)	-4.84	< 0.001 a*
TMT-A score (s)	32.51 (12.11)	24.98 (8.06)	4.47	< 0.001 a*
TMT-B score (s)	83.57 (29.28)	68.02 (29.20)	2.84	0.005 <sup>a*</sup>
PDQ-D	62.63 (15.99)	32.08 (9.05)	14.5 9	< 0.001 a*
<b>Inflammation</b>	-	-	-	-
IL-1 $\beta$ (pg/ ml)	1.71 (0.99, 2.29)	1.66 (1.04, 2.87)	-0.62	0.534 <sup>c</sup>
IL-2 (pg/ ml)	3.59 (2.24, 8.90)	3.63 (2.50, 6.50)	0.55	0.584 <sup>c</sup>
IL-4 (pg/ ml)	1.14 (0.79, 1.83)	1.13 (0.74, 1.95)	0.21	0.835 <sup>c</sup>
IL-5 (pg/ ml)	0.94 (0.51, 1.30)	0.64 (0.36, 1.07)	2.02	0.044 <sup>c*</sup>
IL-6 (pg/ ml)	2.70 (1.78, 3.96)	2.36 (1.45, 3.43)	1.09	0.274 <sup>c</sup>

IL-8 (pg/ ml)	20.89 (11.48, 67.27)	59.58 (29.90, 149.29)	-4.06	< 0.001 <sup>c*</sup>
IL-10 (pg/ ml)	1.78 (1.11, 2.21)	1.40 (1.05, 2.02)	2.17	0.030 <sup>c*</sup>
IL-12p70 (pg/ ml)	1.31 (0.81, 2.50)	1.37 (0.73, 2.50)	0.02	0.984 <sup>c</sup>
IL-17A (pg/ ml)	4.19 (2.59, 15.00)	4.45 (2.15, 13.61)	0.81	0.420 <sup>c</sup>
IFN- $\alpha$ (pg/ ml)	1.29 (0.73, 2.07)	1.07 (0.69, 1.95)	1.02	0.306 <sup>c</sup>
TNF- $\alpha$ (pg/ ml)	1.85 (1.26, 3.70)	1.73 (1.05, 2.76)	1.30	0.193 <sup>c</sup>
TNF- $\beta$ (pg/ ml)	1.41 (0.95, 2.50)	1.39 (0.83, 2.50)	0.65	0.516 <sup>c</sup>
IFN- $\gamma$ (pg/ ml)	1.50 (0.91, 2.51)	1.48 (0.87, 3.57)	0.33	0.742 <sup>c</sup>
hs-CRP (mg/ L)	0.31 (0.20, 1.03)	0.32 (0.20, 0.68)	1.02	0.310 <sup>c</sup>

**Notes:** Mean (SD) or Median (LQ, UQ) were reported. Test indicates test statistic from the corresponding statistical test.

<sup>a</sup>The  $p$ -value was obtained by a two-sample  $t$ -test.

<sup>b</sup>The  $p$ -value was obtained by a  $\chi^2$  test.

<sup>c</sup>The  $p$ -value was obtained by a Mann-Whitney  $U$  test.

\*The asterisk indicates  $p < 0.05$ .

Abbreviations: mFD: mean Frame-wise Displacement; IL: Interleukin; TNF: tumor necrosis factor; INF: interferon; hs-CRP: High-sensitivity C-reactive protein; HAMD: Hamilton depression rating scale; HAMA: Hamilton Anxiety Rating Scale; SHAPS: Snaith-Hamilton Pleasure Scale; DST: Digit Span Test; TMT-A: Trail Making Test Part A; TMT-B: Trail Making Test Part B; PDQ-D: Perceived Deficits Questionnaire-Depression; s: second; SD: standard deviation; LQ: lower quartile; UQ: upper quartile.

**Table 2.** Group differences in DMN functional coupling.

<b>Periodic spatiotemporal coupling</b>	<b>Networks</b>	<b><i>T</i> value</b>	<b><i>P</i> value</b>
<b>DMN - other networks coupling</b>	-	-	-
L_PCC - R_paracentral lobule (L_31a - R_5mv)	DMN A - Ventral attention	-3.42	< 0.001
L_PCC - R_MCC (L_23d - R_23c)	DMN A - Ventral attention	-3.53	< 0.001
R_OFPC - R_MT complex area (R_10d - R_V3CD)	DMN A - Visual peripheral	-3.78	< 0.001
R_PCC - R_ACC (R_31a - R_a32pr)	DMN A - Salience	-3.82	< 0.001
R_sgACC - R_dIPFC (R_s32 - R_i6-8)	DMN A - Control B	4.14	< 0.001
R_IFG - L_IPL (R_45 - L_PGp)	DMN B - Dorsal attention A	-3.44	< 0.001
R_OFC - R_aSTG (R_47m - R_STGa)	DMN B - TPJ	4.67	< 0.001
R_POS - R_FOP (R_POS1 - R_FOP4)	DMN C - Ventral attention	-3.40	< 0.001
R_POS - R_FOP (R_POS1 - R_FOP3)	DMN C - Ventral attention	-3.40	< 0.001
R_PHC - L_FOP (R_H - L_FOP5)	DMN C - Salience	-3.61	< 0.001
<b>Within - DMN coupling</b>	-	-	-
R_mPFC - R_PHC (R_10r - R_H)	DMN A - DMN C	3.39	< 0.001
L_PCC - R_PHC (L_v23ab - R_H)	DMN A - DMN C	3.48	< 0.001

**Notes:** Results are reported using a two-sample *t*-test ( $p < 0.001$ ). Cerebral regions were parcellated using the Glasser 360 atlas. For clarity, regions were denoted using functional shorthand names, with corresponding Glasser labels

provided in parentheses (e.g., R\_mPFC - R\_PHC; R\_10r-R\_H). Network assignments followed the Yeo 17-network parcellation. The MT complex area, located in the lateral occipital cortex, encompasses the motion-sensitive Middle Temporal (MT/V5) region and its neighboring visual areas. Abbreviations: DMN: default mode network; TPJ: Temporo-Parietal Junction; PCC: posterior cingulate cortex; MCC: mid-cingulate cortex; OFPC: orbital frontopolar cortex; MT: middle temporal; ACC: anterior cingulate cortex; sgACC: subgenual anterior cingulate cortex; dlPFC: dorsolateral prefrontal cortex; OFC: orbitofrontal cortex; aSTG: anterior superior temporal gyrus; lFG: inferior frontal gyrus; IPL: inferior parietal lobule; FOP: frontal opercular areas; PHC: parahippocampal; mPFC: medial prefrontal cortex; POS: parieto-occipital sulcus; L, left side of cerebrum; R, right side of cerebrum.

**Table 3.** Moderation analysis of peripheral inflammatory cytokines on differential coupling and behavior in the MDD group.

<b>Moderator variable (M)</b>	<b>Independent variable (X)</b>	<b>Dependent variable (Y)</b>	<b><math>\beta</math> value</b>	<b><math>\Delta R^2</math> value</b>	<b>F value</b>	<b>P value</b>	<b>95% CI</b>
IL-8	R_IFG - L_IPL (R_45 - L_PGp)	TMT-B scores	0.09	0.11	7.41	0.009	[0.02, 0.16]
IL-17A	R_IFG - L_IPL (R_45 - L_PGp)	TMT-B scores	-2.28	0.10	8.59	0.005	[-3.8, -0.7]

**Notes:** Cerebral regions were parcellated using the Glasser 360 atlas. For clarity, regions were denoted using functional shorthand names, with corresponding Glasser labels provided in parentheses (e.g., R\_IFG - L\_IPL; R\_45 - L\_PGp). Abbreviations: IL: interleukin; TMT: Trail Making Test; IFG: inferior frontal gyrus; IPL: inferior parietal lobule; L, left side of cerebrum; R, right side of cerebrum; CI: confidence intervals.

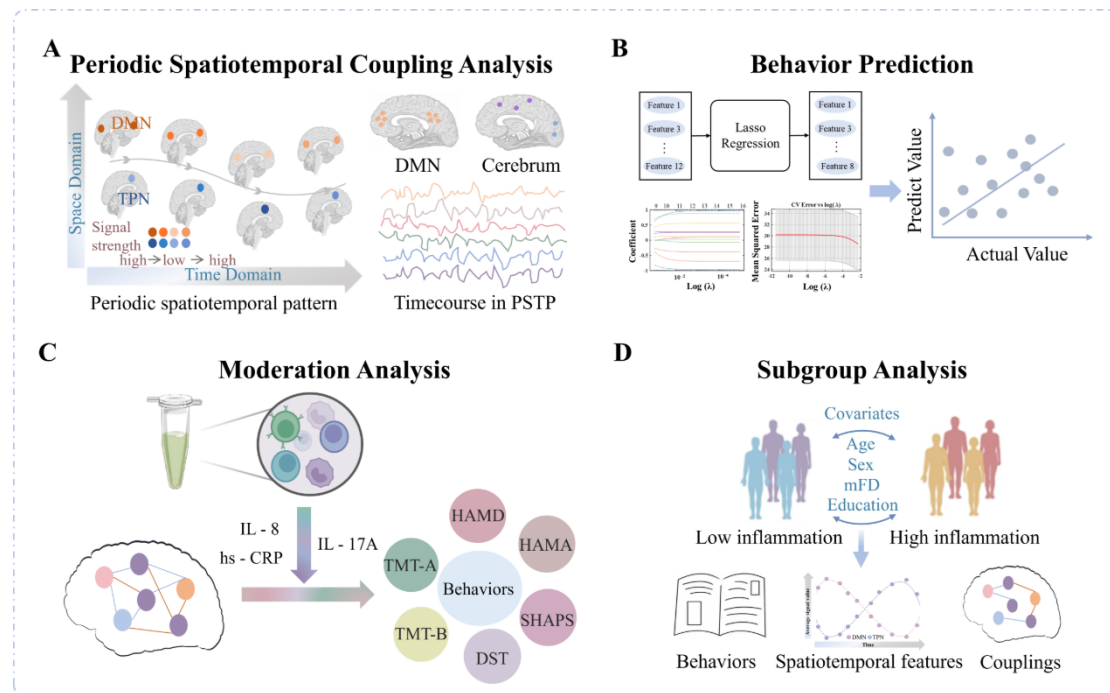


**Fig. 1. Study workflow.** A. The periodic spatiotemporal pattern was identified based on the anti-correlated switching between the DMN and TPN, and DMN functional couplings with cerebral networks were computed using Spearman correlations within this pattern. B. Behavior was predicted using functional couplings that showed significant between-group differences as predictors in a LASSO regression model. C. Peripheral inflammatory cytokines were measured, and moderation analyses were conducted to examine the regulatory effects of inflammation on brain-behavior relationships. D. Cytokines with significant moderating effects were used to divide participants into high- and low-inflammation subgroups. Behavioral performance, dynamic characteristics of PSTP, and functional couplings were then compared across subgroups and HC. Abbreviations: PSTP: periodic spatiotemporal pattern; DMN: default mode network; TPN: task-positive network; IL: Interleukin; hs-CRP: High-sensitivity C-reactive protein; HAMD: Hamilton depression rating scale; HAMA: Hamilton Anxiety Rating Scale; SHAPS: Snaith-Hamilton Pleasure Scale; DST: Digit Span Test; TMT-A: Trail Making Test Part A; TMT-B: Trail Making Test Part B.

## Group Differences in DMN Functional Coupling

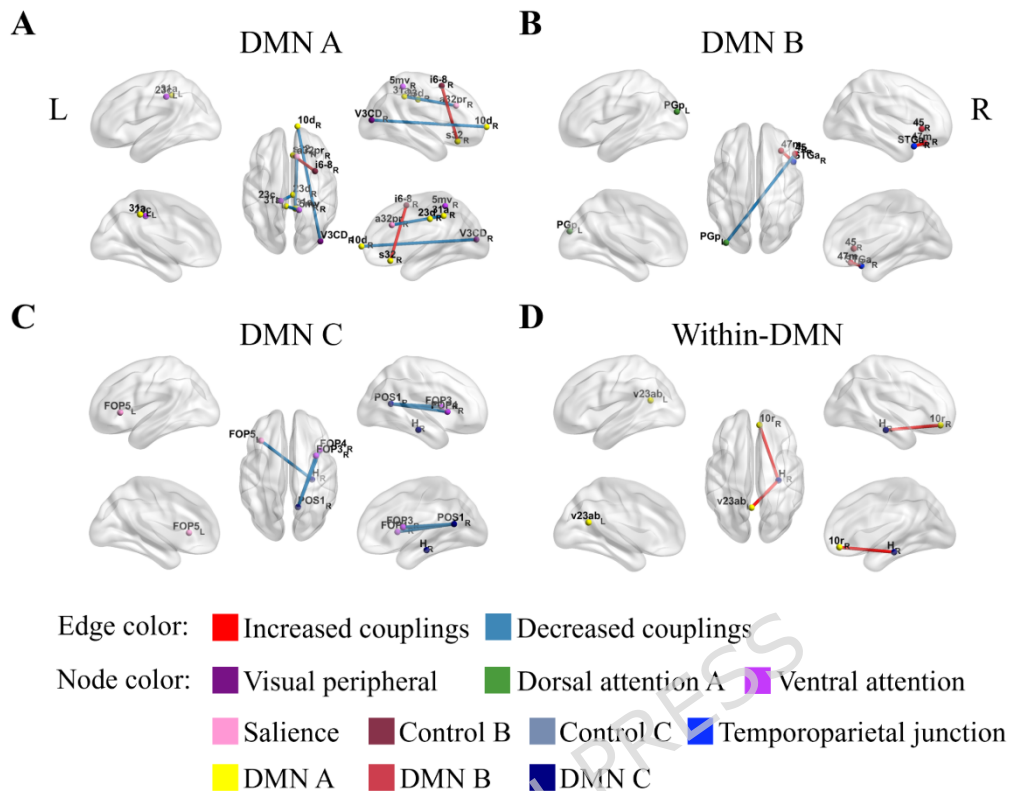


**Fig. 2. Group differences in DMN functional coupling between MDD and HC (two-sample  $t$ -test,  $p < 0.001$ ).** A-C: Differences in coupling between the DMN A/B/C subsystem and other networks. D: Group differences in within-DMN coupling. Red edges indicate increased coupling in MDD relative to HC, while blue edges indicate decreased coupling. Node colors denote different functional networks. Abbreviations: DMN: default mode network; L, left side of cerebrum; R, right side of cerebrum.

### Correlation between DMN Functional Coupling and Behaviors

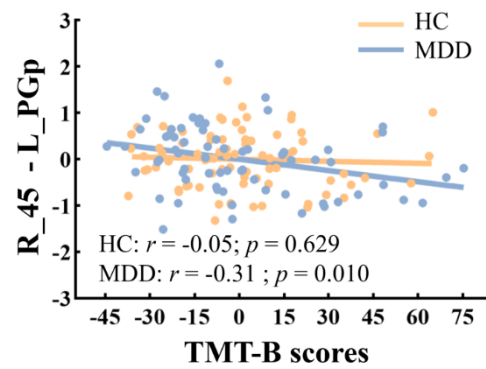


**Fig. 3. Correlation between DMN functional couplings and behaviors in MDD.** Correlation between the R\_45 - L\_PGp and TMT-B scores. Abbreviations: TMT-B: Trail Making Test Part B; L, left side of cerebrum.

## Prediction of Digital Span Test Scores

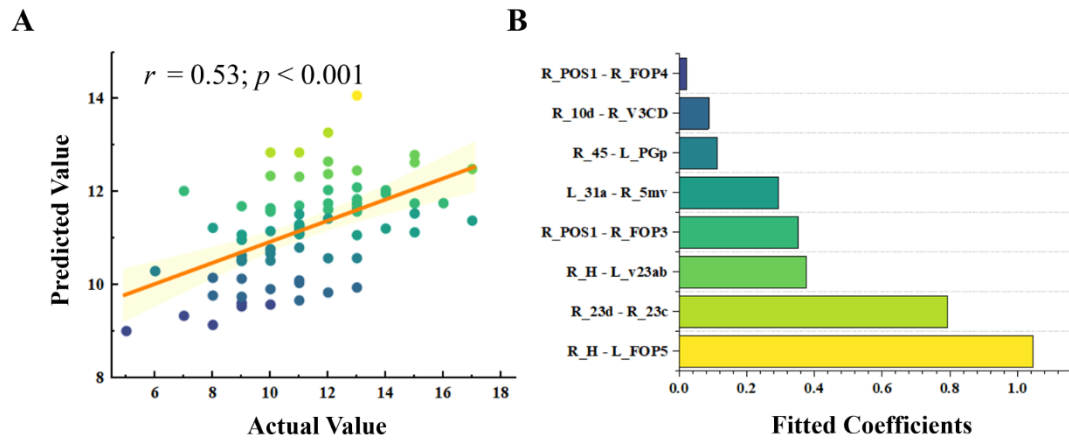


**Fig. 4. Prediction of DST scores in MDD using DMN couplings.** A. Correlation between the actual and predicted DST scores. B. Fitted coefficients of each edge in the LASSO regression. Edges with coefficients of zero are not shown. Abbreviations: DST: digital span test; L, left side of cerebrum; R, right side of cerebrum.

## Moderation Analysis

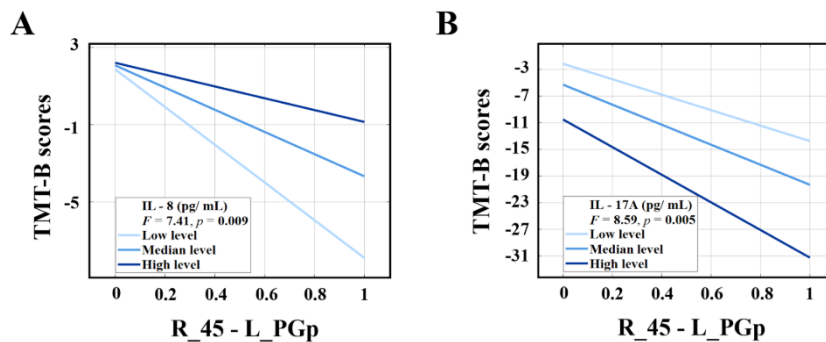


**Fig. 5. Moderation analysis of inflammatory cytokines on the relationship between functional coupling and behavior in MDD.** A. Positive moderating effect of IL-8 on the association between R\_45 - L\_PGp coupling and TMT-B scores. B. Negative moderating effect of IL-17A on the association between R\_45 - L\_PGp coupling and TMT-B scores. Notes: Cerebral regions were parcellated using the Glasser 360 atlas. Abbreviations: IL: Interleukin; TMT-B: Trail Making Test Part B; L, left side of cerebrum; R, right side of cerebrum.

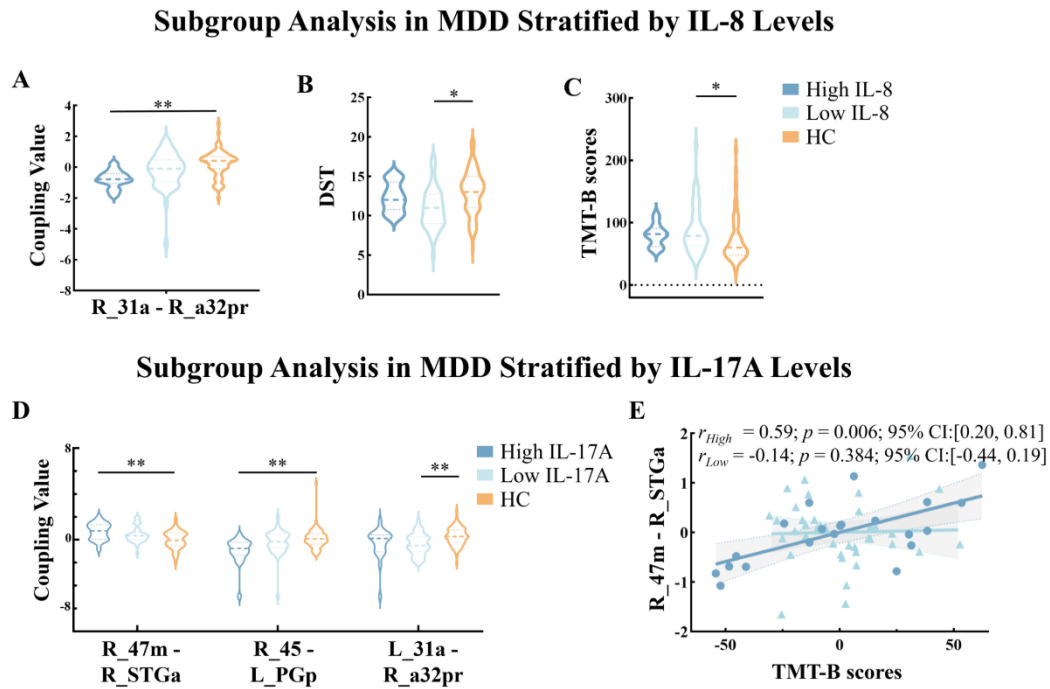


**Fig. 6. Subgroup analysis based on inflammatory cytokines.** A-C. Group differences in DMN coupling and behavioral measures between high- and low-inflammatory subgroups defined by IL-8 levels. D. Results based on subgroup stratification by IL-17A levels. E. Correlations between R\_47m - R\_STGa coupling and HAMD scores in the high and low IL-17A groups. Note: \* Bonferroni-corrected  $p < 0.05$ , \*\* Bonferroni-corrected  $p < 0.001$ . Abbreviations: IL: Interleukin; DST: Digit Span Test; TMT-B: Trail Making Test Part B; CI: confidence intervals; L, left side of cerebrum; R, right side of cerebrum.